THE JOURNAL OF BIOLOGICAL CHEMISTRY
Vol. 279, No. 49, Issue of December 3, pp. 51049–51056, 2004

Printed in U.S.A.

Free Fatty Acid-induced β-Cell Defects Are Dependent on Uncoupling Protein 2 Expression*

Received for publication, August 11, 2004, and in revised form, September 17, 2004
Published, JBC Papers in Press, September 23, 2004, DOI 10.1074/jbc.M409189200

Jamie W. Joseph‡§, Vasilij Koshkin‡¶, Monique C. Saleh‖, William I. Sivitz, Chen-Yu Zhang‡‡, Bradford B. Lowell‡‡, Catherine B. Chan‖, and Michael B. Wheeler‡§§**

*From the ‡Departments of Medicine and Physiology, University of Toronto, Ontario M5S 1A8, Canada, **Divisions of Endocrinology and Metabolism, Department of Internal Medicine, University of Iowa, Iowa City, Iowa 52246, ‖Department of Biomedical Sciences, Atlantic Veterinary College, University of Prince Edward Island, Prince Edward Island C1A4P3, Canada, and ‡‡Division of Endocrinology, Department of Medicine, Beth Israel Deaconess Medical Center and Harvard Medical School, Boston, Massachusetts 02215*

Chronic exposure to elevated free fatty acids (lipotoxicity) induces uncoupling protein (UCP2) in the pancreatic β-cell, and therefore a causal link between UCP2 and β-cell defects associated with obesity may exist. Recently, we showed that lipid treatment *in vivo* and *in vitro* in UCP2(−/−) mice/islets does not result in any loss in β-cell glucose sensitivity. We have now assessed the mechanism of maintained β-cell function in UCP2(−/−) mice by exposing islets to 0.4 mM palmitate for 48 h. Palmitate treatment increased triglyceride concentrations in wild type (WT) but not UCP2(−/−) islets because of higher palmitate oxidation rates in the UCP2(−/−) islets. Dispersed β-cells from the palmitate-exposed WT islets had reduced glucose-stimulated hyperpolarization of the mitochondrial membrane potential compared with both control WT and palmitate-exposed UCP2(−/−) β-cells. The glucose-stimulated increases in the ATP/ADP ratio and cytosolic Ca^{2+} are attenuated in palmitate-treated WT but not UCP2(−/−) β-cells. Exposure to palmitate reduced glucose-stimulated insulin secretion (GSIS) in WT islets, whereas UCP2(−/−) islets had enhanced GSIS. Overexpression of recombinant UCP2 but not enhanced green fluorescent protein in β-cells resulted in a loss of glucose-stimulated hyperpolarization of the mitochondrial membrane potential and GSIS similar to that seen in WT islets exposed to palmitate. Reactive oxygen species (ROS) are known to increase the activity of UCP2. We showed that ROS levels were elevated in control UCP2(−/−) islets as compared with WT and UCP2(−/−) islets overexpressing UCP2 and that palmitate increased ROS in WT and UCP2(−/−) islets overexpressing UCP2 but not in UCP2(−/−) islets. Thus, UCP2(−/−) islets resisted the toxic effects of palmitate by maintaining glucose-dependent metabolism-secretion coupling. We propose that higher free fatty acid oxidation rates prevent accumulation of triglyceride in UCP2(−/−) islets, such accumulation being a phenomenon associated with lipotoxicity.

In the pancreatic β-cell, glucose is metabolized by glycolysis producing pyruvate and nicotinamide adenine dinucleotide (NADH), both of which are transported into the mitochondria where pyruvate is metabolized by the tricarboxylic acid cycle to produce NADH and flavin adenine dinucleotide ($FADH_2$). Both cytosolic and mitochondrial sources of NADH along with mitochondrial $FADH_2$ stimulate the electron transport chain (complexes I–IV) to pump H^+ ions out of the mitochondrial matrix, thereby hyperpolarizing the inner mitochondrial membrane and generating the proton-motive force used to generate ATP by ATP synthase (1). Mitochondrial ATP production from glucose is the key modulator of glucose-stimulated insulin secretion (GSIS),[1] and mitochondrial oxidative metabolism has been estimated to produce 98% of β-cell ATP (1).

The members of the uncoupling protein (UCP) family are involved in regulating cellular ATP production and are localized to the inner mitochondrial membrane (2). Uncoupling protein-1, -2, and -3 share a high degree of homology and are expressed in a tissue-specific manner (3). Data from several laboratories support a role for UCPs as "typical" uncouplers (4, 5) that modulate the efficiency of ATP production (3) by catalyzing the translocation of protons across the mitochondrial membrane to reduce the proton-motive force (4, 5). Moreover, UCP2 mediates proton leak within the normal environment of intact cells (6). UCP2 is the only known uncoupling protein expressed in pancreatic β-cells (7).

The human UCP2 promoter polymorphism −866 G/A is associated with a greater risk of obesity in Caucasians (8). Type 2 diabetic patients homozygous for the −866A allele polymorphism require a higher frequency of insulin treatments and have significantly lower glucose-induced insulin secretion (9). Individuals with the −866 A/A genotype also have enhanced UCP2 transcriptional activity and elevated UCP2 expression (10). Human islets isolated from −866 A/A donors have lower GSIS than those isolated from −866 G/A heterozygous and G/G homozygous individuals (10). In addition, increased UCP2 expression in individuals with the homozygous −866 A allele is associated with a reduction in oxidative stress and coronary heart disease (11). These human studies suggest that the var-

* This work was supported in part by Operating Grant MOP-12898 from the Canadian Institutes of Health Research (CIHR) (to M. B. W. and C. B. C.). The costs of publication of this article were defrayed in part by the payment of page charges. This article must therefore be hereby marked "*advertisement*" in accordance with 18 U.S.C. Section 1734 solely to indicate this fact.

§ Supported by a CIHR doctoral award.

¶ Supported by a New Emerging Teams Grant in Diabetes Complications from CIHR.

§§ Supported by a CIHR investigator award. To whom correspondence should be addressed: University of Toronto, Dept. of Physiology, 1 Kings College Circle, Rm. 3352, Toronto, Ontario M5S 1A8, Canada. Tel.: 416-978-6737; Fax: 416-978-4940; E-mail: michael.wheeler@utoronto.ca.

[1] The abbreviations used are: GSIS, glucose-stimulated insulin secretion; UCP, uncoupling protein; WT, wild type; HFD, high fat diet; FFA, free fatty acids; ROS, reactive oxygen species; $\Delta\Psi_m$, mitochondrial membrane potential; FCCP, carbonyl cyanide *p*-(trifluoromethoxy) phenylhydrazone; KRBH, Krebs-Ringer-bicarbonate-HEPES; TG, triglycerides; DCF, 2′,7′-dichlorodihydrofluorescein diacetate; GAPDH, glyceraldehyde-3-phosphate dehydrogenase; Rh123, rhodamine 123; MnTBAP, Mn(III) tetrakis-(4-benzoic acid) porphyrin; EGFP, enhanced green fluorescent protein; EYFP, enhanced yellow fluorescent protein.

iation seen in insulin secretion from individual to individual may be in part due to the −866 G/A UCP2 promoter polymorphism and that increased UCP2 can attenuate GSIS by altering substrate oxidation.

Induction of pancreatic β-cell UCP2 *in vivo* and *in vitro* has a negative impact on GSIS, likely by limiting increases in ATP production following dissipation of the proton gradient generated by glucose metabolism (12–14). What regulates UCP2 and the physiological role of this protein in the pancreatic β-cell are not well understood. It is known that free fatty acids (FFA) and reactive oxygen species (ROS) increase the expression and activity of UCP2 (5, 15). This is an important interaction because increased FFA metabolism leads to an increase in energy flux through the electron transport chain, which can lead to an increase in the production of ROS in β-cells (16, 17). UCP2 may be involved in this interaction by limiting the FFA-stimulated increase in ROS production by dissipating the excess energy (15). However, ROS-mediated activation of UCP2 is now thought to be an important determinant of impaired GSIS (18). We propose that UCP2 may play a protective role in the β-cell by mitigating the consequences of excess FFA- and glucose-induced ROS production. However, in protecting from ROS the increased β-cell UCP2 activity down-regulates GSIS.

Previously, we used a well characterized *in vivo* model in which mice were treated with a high fat diet (HFD) for 4.5 months, and we found that UCP2(−/−) mice were resistant to the effects of a HFD in terms of β-cell function. To understand the cellular responses of UCP2(−/−) β-cells to FFA, we utilized a well known *in vitro* model of lipotoxicity in which isolated islets or dispersed β-cells were treated with control medium or medium containing 0.4 mM palmitate for 48 h (6, 13). We then examined a number of key metabolic parameters involved in GSIS including insulin content, FFA metabolism, mitochondrial membrane potential, ATP/ADP ratio, cytosolic Ca^{2+} changes, and insulin secretion. We showed that UCP2(−/−) islets had no alterations in mitochondrial membrane potential, ATP/ADP ratio, and cytosolic Ca^{2+} responses after palmitate treatment, whereas wild type (WT) islets showed dysfunctional responses. We also found that palmitate did not increase ROS in UCP2(−/−) β-cells. Therefore UCP2(−/−) mice maintained robust glucose-dependent metabolism-secretion coupling after FFA exposure that reverted to a WT islet phenotype after UCP2 overexpression in UCP2(−/−) islets.

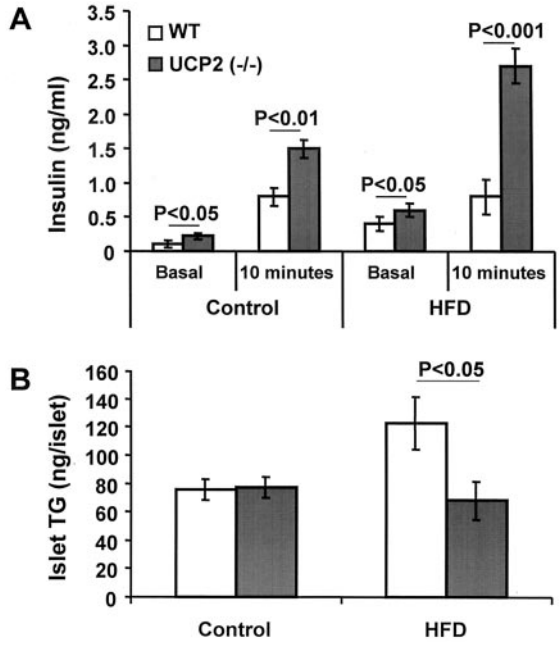

FIG. 1. **Insulin secretion and islet triglycerides in WT and UCP2(−/−) mice after a HFD.** *A*, plasma insulin response of WT and UCP2(−/−) mice after an intraperitoneal glucose tolerance test. Insulin secretion was measured prior to intraperitoneal glucose tolerance test (*basal*) and 10 min after the intraperitoneal glucose injection (*10 min*). *B*, triglyceride content of islets from WT mice or from UCP2(−/−) mice after treatment with a control diet or a high fat diet for 4.5 months ($n = 6$).

EXPERIMENTAL PROCEDURES

Reagents—Carbonyl cyanide *p*-(trifluoromethoxy) phenylhydrazone (FCCP), ATP sulfurylase, pyruvate kinase, collagenase type V and type XI, ATP luciferase, D-luciferin, ATP, and ADP were all purchased from Sigma.

Animals—Male UCP2 (WT) or UCP2 knockout (−/−) mice at 4 months of age were used in the present study and were bred from lines generated as described previously (13, 14). For the HFD studies, half of the mice were placed on either a control diet (rodent diet 8664, Harlan Teklad, Madison, WI) or a HFD (D12451, Research Diets Inc., New Brunswick, NJ). The fat source was lard, comprising 45% of the total calories. The mice remained on the HFD or control diet for 4.5 months (13). Intraperitoneal glucose tolerance tests were performed as described previously (14). Plasma insulin levels were determined using a rat insulin enzyme-linked immunosorbent assay kit (Crystal Chem, Chicago, IL).

Adenoviral Vectors—Adenoviral vectors used in these studies are described elsewhere and include adenovirus expressing UCP2 (AdUCP2) (12), adenovirus expressing enhanced yellow fluorescent protein driven by the rat insulin promoter-2 (AdRIP2EYFP) (19), and adenovirus expressing enhanced green fluorescent protein driven by a cytomegalovirus promoter (AdEGFP) (7). Adenovirus-mediated overexpression of enhanced green fluorescent protein (EGFP) was used as a control for the overexpression of UCP2 using AdUCP2.

Real-time PCR Analysis of UCP2 mRNA Expression—UCP2 mRNA levels were detected by real-time PCR as described (13). Briefly, UCP2- and GAPDH-specific fluorescent probes were obtained from Biosearch Technologies Inc. (Novato, CA) (13). UCP2 and GAPDH expression levels were measured simultaneously using a Taqman Universal PCR master mix and an ABI Prism 7900HT sequence detection system (Applied Biosystems, Branchburg, NJ). All mRNA levels were quantified using a standard curve of a known amount of mouse cDNA (cDNAs were created from forward and reverse primers (13)). All cDNA PCR products that were used in the standard curve were purified using a MinElute PCR purification kit (Qiagen, Mississauga, Ontario, Canada). The real-time PCR conditions were 2 min at 50 °C, 10 min at 95 °C, and then 40 cycles for 15 s at 95 °C and 1 min at 53 °C. UCP2 mRNA levels were corrected for GAPDH levels by dividing UCP2 mRNA levels by GAPDH mRNA levels. There were no differences in GADPH levels between treatments.

Western Blot Analysis of UCP2 Protein Expression—Ambient and virally induced expression of UCP2 was assessed by immunoblotting. UCP2 was detected using goat anti-UCP2 antibody (Research Diagnostic Inc., 1:400), and the secondary antibody was peroxidase-conjugated donkey anti-goat (Jackson Immunoresearch, 1:5000).

Pancreatic Islet Isolation—Pancreatic islets were isolated as described previously (13, 14, 20). Briefly, the pancreatic duct was perfused with 3 ml of collagenase (3 mg/ml). The pancreas was then chopped into 2-mm pieces and digested by shaking (50 rpm) for 10–15 min at 37 °C. Islets were partially isolated by sedimentation and then hand picked from the acinar tissue debris.

Islet Dispersion—Freshly isolated islets were incubated for 8–9 min at room temperature in Krebs-Ringer-bicarbonate-HEPES (KRBH) buffer with 1 mM EDTA, 0.2% (w/v) bovine serum albumin, and 5.6 mM glucose. KRBH buffer contained (in mM) 118 NaCl, 4.4 KCl, 1.2 $MgCl_2$, 1.5 KH_2PO_4, 5 $NaHCO_3$, and 10 HEPES, pH 7.4. Islets were further incubated in KRBH buffer containing 1 mM EDTA, trypsin (25 μg/ml, Sigma), and DNase I (2 μg/ml, Sigma) at 37 °C for 9 min with gentle pipetting every 2 min. The cells were washed twice in the islet culture medium RPMI (Roswell Park Memorial Institute) supplemented with 5.6 mM glucose, 0.25% HEPES (Sigma), 20 units/ml penicillin G sodium, and 20 μg/ml streptomycin sulfate (Invitrogen). Cells were then plated onto collagen-coated glass cover slips and allowed to attach overnight in islet culture medium containing 10% fetal bovine serum (Invitrogen).

Islet and Dispersed β-Cell Culture—Islets and dispersed β-cells were

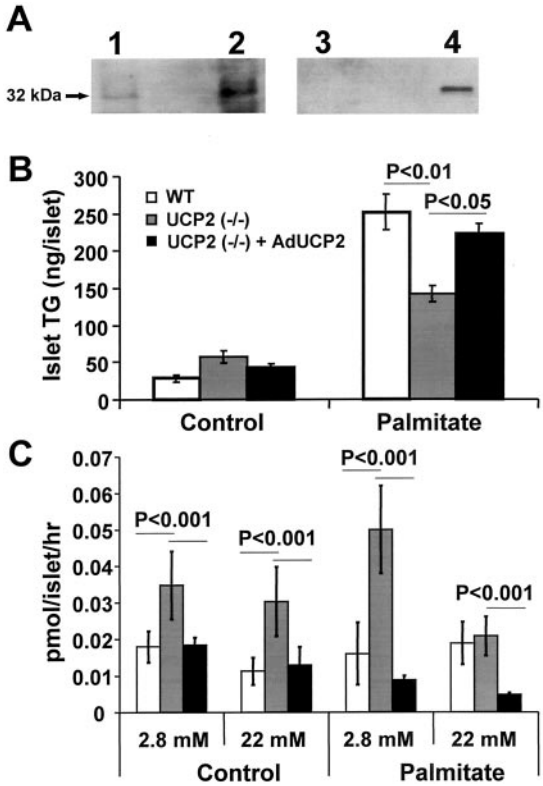

FIG. 2. **UCP2 expression, triglyceride content, and β-oxidation of WT, UCP2(−/−), and UCP2(−/−) islets infected with AdUCP2 after being cultured in control medium or 0.4 mM palmitate medium for 48 h.** *A*, Western blot analysis of endogenous and adenovirus-driven overexpression of UCP2. *Lane 1*, WT mouse islets cultured in control medium for 48 h; *lane 2*, WT mouse islets cultured in 0.4 mM palmitate for 48 h; *lane 3*, UCP2(−/−) islets cultured with control medium; *lane 4*, UCP2(−/−) mouse islets infected with AdUCP2 (n = 2–3). *B*, triglyceride content of islets after treatment ($n > 6$). *C*, β-oxidation of islets after treatment ($n > 7$). Islets were studied in response to either low glucose (2.8 mM glucose) or high glucose (22 mM glucose).

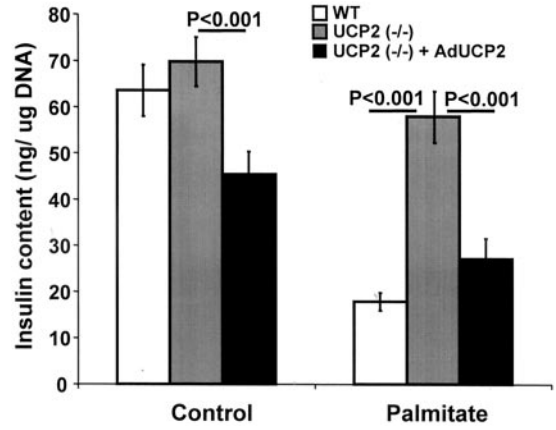

FIG. 3. **Insulin content of islets treated with either control medium or medium containing 0.4 mM palmitate for 48 h.** Islets were from either wild type mice (*WT*), UCP2(−/−) mice (*UCP2(−/−)*), or UCP2(−/−) mice overexpressing UCP2 (*UCP2(−/−) + AdUCP2*) ($n > 14$).

preincubated for 24 h in islet culture medium containing 10% (v/v) fetal bovine serum and then transferred to control medium (culture medium with 5% (v/v) fetal bovine serum and 0.25% (w/v) bovine serum albumin without free fatty acids (Sigma)) or palmitate medium (control medium with 0.4 mM palmitate) for 48 h. In some experiments using UCP2(−/−) islets or dispersed β-cells, UCP2 was reintroduced using AdUCP2 at the beginning of the 48-h culture period at a multiplicity of infection of 5×10^3.

Islet Triglyceride Measurements—Triglycerides (TG) were extracted from groups of 100 islets by lipid extraction in a chloroform/methanol (2:1 v/v) mixture as described elsewhere (21, 22). For the assay, the dry material derived from evaporation of the chloroform phase was resuspended in water in the presence of a detergent (Thesit or polidocanol (Sigma) 20% w/v in chloroform). TGs were measured enzymatically with a commercial kit (GPO Trinder; Sigma). Triolein (Sigma), which was dissolved in chloroform/methanol and processed similarly to samples, was used as the standard.

Islet β-Oxidation—Palmitate oxidation in isolated islets was measured as described previously (23). In brief, 50 islets per condition were incubated in KRBH experimental medium containing 2.8 or 22 mM glucose, 1% fatty acid-free bovine serum albumin, 0.8 mM carnitine, and 1 μCi of [^{14}C]palmitate (Amersham Biosciences) for 2 h at 37 °C in an orbital water bath (100 cycles/min). The reaction was stopped by the addition of perchloric acid, and the evolved $^{14}CO_2$ was captured with hyamine hydroxide with shaking for an additional 2 h.

Mitochondrial Membrane Potential Imaging—Glucose-induced changes in mitochondrial membrane potential ($\Delta\Psi_m$) were quantified in dispersed β-cells. After the 48-h treatment period, cells were loaded with rhodamine 123 (2.6 μM Rh123 for 15 min) (Molecular Probes, Eugene, OR). Fluorescence was excited at 490 nm and measured at 530 nm. All membrane potential measurements were done at 37 °C. Images were captured and analyzed using the Merlin software (Olympus America, Life Sciences Resources, Melville, NY) as described elsewhere (13, 24). Exposure time was 0.2 s, and images were acquired at ~0.2 Hz. Rh123 is a fluorescent lipophilic cationic dye that specifically partitions into negatively charged mitochondrial membranes. Under these Rh123 loading conditions, hyperpolarization of the $\Delta\Psi_m$ as seen after nutrient stimulation results in an increase in the Rh123 concentration in the mitochondrial membrane, leading to an aggregation of dye molecules and quenching of the fluorescence signal. Conversely, depolarization of $\Delta\Psi_m$ allows the dye to redistribute from the mitochondria into the cytosol, resulting in an increase of the Rh123 signal (25). Changes in fluorescence from 2.8 to 20 mM glucose were determined by comparison with the average base-line fluorescence over the first 50 s, which was arbitrarily assigned a value of 1.0. Assessment of the glucose-induced changes was done by averaging data between 500–700 s and comparing the normalized values to the base line. At the end of an experiment 1 μM FCCP was added to assess cell viability and to test the ability of the cell loaded with Rh123 to respond to changes in the $\Delta\Psi_m$ induced by the chemical uncoupler.

Islet GSIS, ADP, and ATP Determination—Groups of 25 islets were preincubated in experimental medium for two sequential 30-min periods at 37 °C, 5% CO_2. Islets were then incubated for 2 h at the indicated glucose concentration (either 2.8 or 16.7 mM glucose) to assess insulin secretion. Islet DNA and insulin secretion measurements were performed as described previously (13). Islet ATP and ADP content was determined using these same islets at the end of the 2-h incubation period using the method of Tornheim and co-workers (26). In brief, islet ATP and ADP were extracted from the 25 islets with 20 units of 10% (w/v) perchloric acid. After centrifugation, the supernatants were neutralized with 2 N KOH, 0.5 M triethanolamine and then freeze-dried (SpeedVac). Aliquots of each deproteinized sample were assayed for ATP directly with luciferase (Sigma). Other aliquots were treated with ATP sulfurylase in the presence of molybdate to hydrolyze the endogenous ATP to AMP and PP_i. After boiling the samples to inactivate the sulfurylase, ADP was then converted to ATP with pyruvate kinase and phosphoenolpyruvate for measurement with luciferase.

Islet Insulin Content Measurements—At the end of a GSIS experiment and after extracting ATP and ADP, insulin was solubilized from the perchloric acid protein pellet by adding 0.5 N NaOH and heating to 60 °C for 10 min and then neutralized with 2 N HCl. Insulin secretion and insulin content were determined as described previously (27, 28).

Ca^{2+} Imaging—Ca^{2+} imaging was performed on dispersed β-cells plated on collagen-coated cover slips. Data collection was performed with the same equipment used for Rh123 imaging. After dispersion, cells were infected with AdRIP2EYFP and then cultured with either control or palmitate medium for 48 h. Cells were then loaded with 1 μM Fura-2/AM (Molecular Probes) for 45 min at 37 °C. β-Cells were identified using the fluorescence of the EYFP driven by the rat insulin promoter (excitation 490 nm, emission 530 nm). Experiments were performed at 37 °C. Images were obtained with 340- and 380-nm excitation and a 510-nm cutoff emission filter. Exposures lasted 0.2 s, and images were acquired at ~0.2 Hz. Images were collected and analyzed using the Merlin software (13). Data were averaged, and the standard error of the mean was plotted for data points every 40 s.

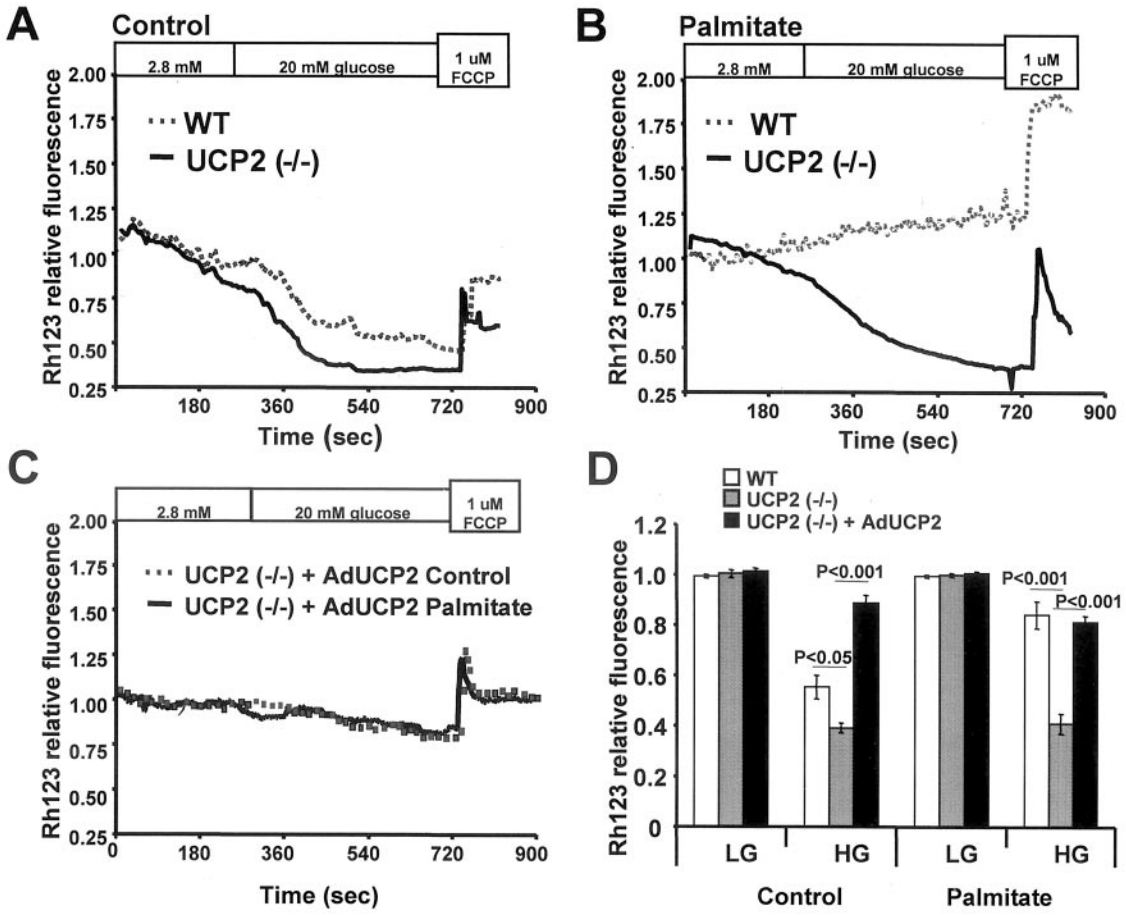

FIG. 4. **Glucose-stimulated alterations in the mitochondrial membrane potential.** Dispersed β-cells from WT or UCP2(−/−) islets treated for 48 h with either control or 0.4 mM palmitate medium. Mitochondrial membrane potential was then studied by loading cells with rhodamine 123. Glucose was applied at 250 s and FCCP at 730 s. *A–C* are representative rhodamine 123 responses from a single β-cell. *A*, control medium-treated islets from WT mice or UCP2(−/−) mice; *B*, islets from WT or UCP2(−/−) mice cultured in 0.4 mM palmitate; *C*, islets from UCP2(−/−) mice overexpressing UCP2 treated with either control medium or medium containing 0.4 mM palmitate. *D*, average responses to high glucose (data were analyzed as described under "Experimental Procedures"). For each set of experiments, at least four different mice were used giving a total of more than 30 cells. *LG*, low glucose; *HG*, high glucose.

Reactive Oxygen Species—ROS were detected in islets using 2′,7′-dichlorodihydrofluorescein diacetate (DCF) (Sigma). Islets were loaded with 10 μM dye in KRBH buffer (containing 5.6 mM glucose) for 20 min at room temperature. Fluorescence of oxidized dye, reflecting cellular oxidation status, was measured with the equipment used for rhodamine 123 imaging (excitation/emission wavelengths 495/530 nm) in KRBH buffer in the presence of 5.6 mM glucose. Images were collected in 30-s intervals with 150-ms exposures and minimal intensity of exciting light. Islet ROS was quantified using standard curves obtained with solutions of the oxidized probe DCF.

Statistics—Statistical significance was assessed by using either Student's *t* test or one-way or two-way analysis of variance for repeated measures followed by multiple Bonferroni comparisons. All data are expressed as means ± S.E.

RESULTS

Islet Triglyceride, β-Oxidation, and Insulin Content—Increased islet TG are associated with an inhibition of GSIS. To ascertain the effects of a HFD on islet TG levels *in vivo*, mice were fed a HFD for 4.5 months (13). To confirm our previous results, where enhanced insulin secretion in UCP2(−/−) mice was observed after a HFD, an intraperitoneal glucose tolerance test was performed. Both basal and glucose-stimulated (10 min after intraperitoneal injection of glucose) insulin levels were significantly higher in UCP2(−/−) mice on the control or the HFD (Fig. 1*A*). There was no difference in islet TG concentrations between islets from WT and UCP2(−/−) mice on the control diet (Fig. 1*B*). After HFD treatment, WT islets had increased TG content compared with UCP2(−/−) islets (Fig. 1*B*).

No detectable UCP2 mRNA or protein levels could be identified in UCP2(−/−) mouse islets infected with either no virus or a control adenovirus (AdEGFP) or when treated with 0.4 mM palmitate (data not shown). Culture of WT islets in 0.4 mM palmitate for 48 h increased UCP2 mRNA expression levels 8-fold over WT control medium-treated islets (UCP2/GAPDH ratio of 0.0372 ± 0.0013 *versus* 0.0047 ± 0.0001, respectively). UCP2 protein levels were also increased in palmitate-treated WT islets (Fig. 2*A*). In UCP2(−/−) islets, AdUCP2 increased UCP2 mRNA expression levels 435-fold over WT control medium-treated islets (UCP2/GAPDH ratio of 2.030 ± 0.2891 *versus* 0.0047 ± 0.0001, respectively). AdUCP2 increased UCP2 protein levels in UCP2(−/−) islets as determined by Western blotting (Fig. 2*A*).

In the *in vitro* study in which islets were exposed to 0.4 mM palmitate for 48 h, islet TG content was not different between the groups of islets (WT, UCP2(−/−), and UCP2(−/−) overexpressing UCP2) treated with control medium (Fig. 2*B*). There was a significant increase in islet TG content in WT, UCP2(−/−), and UCP2(−/−) islets overexpressing UCP2 after treatment with 0.4 mM palmitate, but the degree of increase was significantly lower in the UCP2(−/−) islets treated with

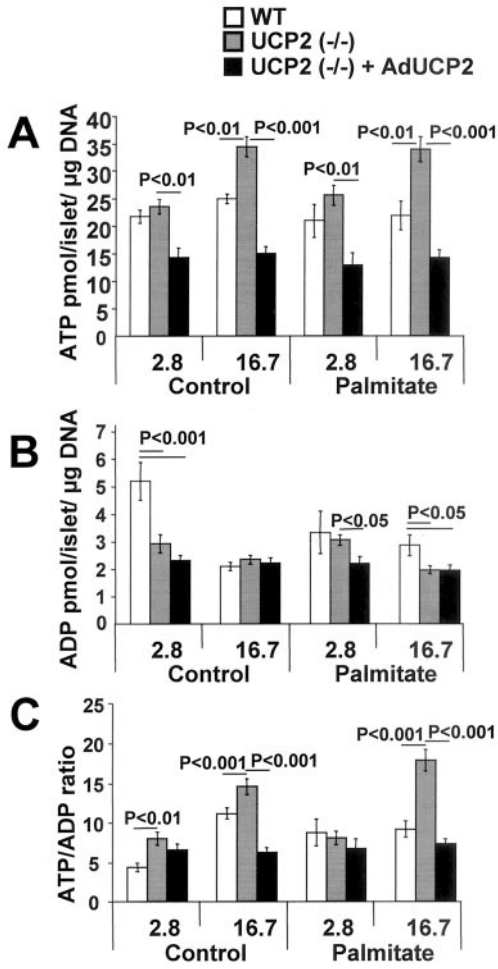

FIG. 5. **Glucose-stimulated increases in ADP, ATP, and ATP/ADP ratio of islets treated with either control medium or medium containing 0.4 mM palmitate (48 h).** Islets were from either WT mice, UCP2(−/−) mice or UCP2(−/−) mice overexpressing UCP2 (*UCP2(−/−) + AdUCP2*). Islets were exposed to either 2.8 or 16.7 mM glucose. *A*, islet ATP content. *B*, islet ADP content. *C*, islet ATP/ADP ratios ($n > 14$).

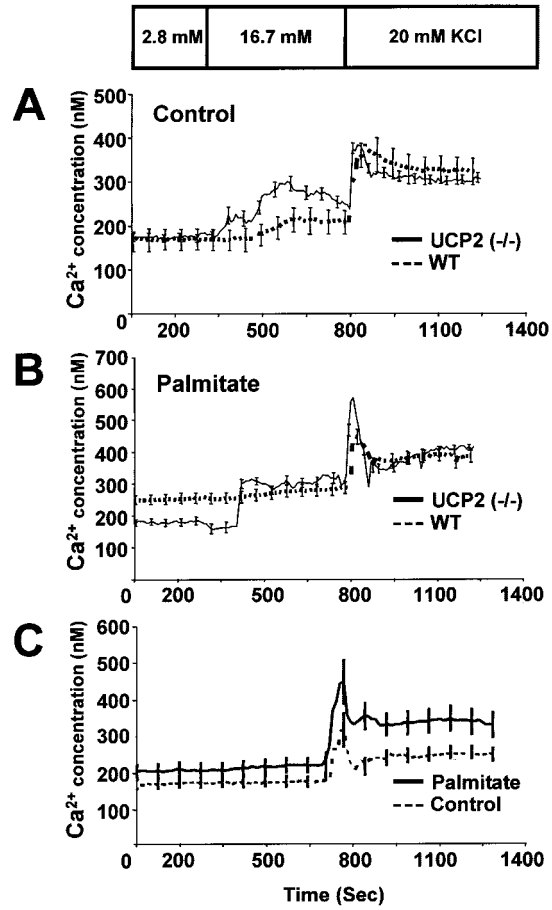

FIG. 6. **Glucose-stimulated alterations in the cytosolic Ca^{2+}.** Mouse islet dispersed β-cells from WT or UCP2 (−/−) mice were treated with control medium or 0.4 mM palmitate for 48 h and then loaded with 1 μM Fura-2 to measure cytosolic Ca^{2+} concentrations. Glucose was applied at 250 s and KCl at 720 s. Traces represent averaged Ca^{2+} data from at least four mice with more than 30 cells/group. S.E. was plotted every 40 s. *A*, control medium-treated islets from WT or UCP2(−/−) mice. *B*, islets from WT or UCP2(−/−) mice treated with 0.4 mM palmitate. *C*, islets from UCP2(−/−) mice overexpressing UCP2 treated with either control medium or medium containing 0.4 mM palmitate (48 h).

palmitate than in the WT and UCP2(−/−) islets overexpressing UCP2 (Fig. 2*B*).

β-Oxidation was significantly increased in UCP2(−/−) islets after treatment with both control medium and palmitate compared with WT islets (Fig. 2*C*). Overexpression of UCP2 resulted in a significant reduction in β-oxidation in UCP2(−/−) islets compared with the UCP2(−/−) control and palmitate treatment groups (Fig. 2*C*). Insulin content of WT islets treated with palmitate was reduced by 71% when compared with control WT islets (Fig. 3). UCP2(−/−) islet insulin content was not affected by treatment with palmitate; however, recovery of UCP2 expression with AdUCP2 resulted in a 52% reduction in insulin content. Importantly, adenovirally mediated overexpression of EGFP, using AdEGFP, did not affect insulin content in UCP2(−/−) islets treated with either control or palmitate (65.3 ± 15.2 and 55.6 ± 16.3 ng of insulin/μg of DNA, respectively, $n = 3$).

Glucose-stimulated Alterations in the Mitochondrial Membrane Potential—We next assessed the ability of UCP2 to alter glucose-stimulated hyperpolarization of the mitochondrial membrane potential. Because the excitation and emission wavelengths of EYFP and Rh123 overlapped, single dispersed β-cell measurements were performed in large islet cells, which were more likely to be β-cells than other islet cell types (29). In all Rh123 experiments, large β-cell-like cells were assessed for responsiveness by application of 1 μM FCCP. Normally, energy substrates lead to a hyperpolarization of the $\Delta\Psi_m$. Glucose stimulated a hyperpolarization of the $\Delta\Psi_m$ in both control WT and UCP2(−/−) β-cells. UCP2(−/−) β-cells hyperpolarized faster and to a greater degree than WT β-cells under control conditions (Fig. 4, *A* and *D*). After treatment with 0.4 mM palmitate, WT β-cells lost their ability to respond to glucose, whereas UCP2(−/−) islets maintained their response (Fig. 4, *B* and *D*). In UCP2(−/−) β-cells expressing AdUCP2 (control or palmitate groups), there was no response in $\Delta\Psi_m$ to glucose (Fig. 4, *C* and *D*). All cells identified as having β-cell-like characteristics were grouped together, and the ability of glucose to hyperpolarize the membrane was averaged (Fig. 4*D*).

Glucose-stimulated Increases in ADP, ATP, and ATP/ADP—ATP levels were significantly elevated in UCP2(−/−) compared with WT islets only under high glucose conditions (Fig. 5*A*). Overexpression of UCP2 in UCP2(−/−) islets significantly reduced ATP content in control and 0.4 mM palmitate-treated islets at both low and high glucose concentrations. Control islet ADP content was significantly decreased in UCP2(−/−) islets and UCP2(−/−) islets overexpressing UCP2 at low glucose, compared with WT islets (Fig. 5*B*). There were no differences in control islets at the high glucose condition. After treatment

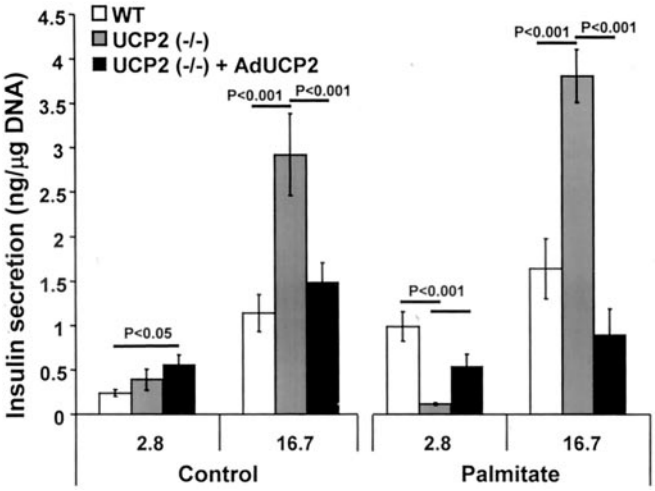

FIG. 7. **Glucose-stimulated insulin release of islets after treatment with either control medium or medium containing 0.4 mM palmitate (48 h).** Islets were from either WT mice, UCP2(−/−) mice, or UCP2(−/−) mice overexpressing UCP2 ($n > 14$).

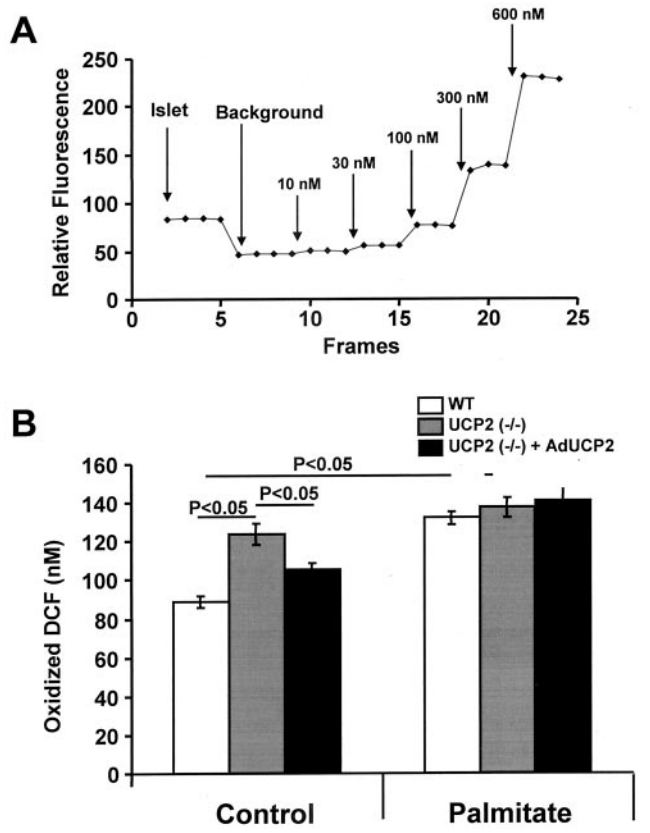

FIG. 8. **Reactive oxygen species production in islets.** *A*, representative fluorescent trace shows steady state level of DCF fluorescence in the islet (initial segment) followed by fluorescence levels corresponding to 0, 10, 30, 100, 300, and 600 nM oxidized DCF. *B*, concentrations of dichlorofluorescein formed from dichlorodihydrofluorescein in WT, UCP2(−/−), and UCP2(−/−) islets overexpressing UCP2 after being treated with control medium or 0.4 mM palmitate for 48 h (n = 5–10 islets).

with palmitate for 48 h, UCP2(−/−) islets had reduced ADP levels after exposure to high glucose compared with WT islets. In addition, palmitate-treated UCP2(−/−) islets overexpressing UCP2 had significantly lower ADP levels at both low and high glucose (Fig. 5*B*).

UCP2(−/−) islets had enhanced glucose-stimulated increases in the ATP/ADP ratio compared with WT islets (Fig. 5*C*). When UCP2(−/−) islets were transduced with AdUCP2, the enhancement of glucose-stimulated increases in the ATP/ADP was lost. After treatment with palmitate, the ability of WT islets and UCP2(−/−) islets overexpressing UCP2 to increase the ATP/ADP in response to glucose was attenuated, whereas UCP2(−/−) islets maintained this ability (Fig. 5*C*). Overexpression of EGFP with AdEGFP had no effect on glucose-stimulated increase in the ATP/ADP ratio in control medium or palmitate-treated UCP2(−/−) islets (18.0 ± 3.3 and 17.5 ± 3.3 respectively, n = 3).

Glucose-stimulated Increases in Cytosolic Ca^{2+} Levels—AdRIP2EYFP was used to identify β-cells from dispersed mouse islets in experiments involving Ca^{2+} imaging with Fura-2. There was no overlap between Fura-2 and EYFP emission when excited with the appropriate wavelengths ((19) and data not shown). In these studies, data were expressed as averaged cytosolic Ca^{2+} responses in EYFP-identified dispersed β-cells. Under control medium conditions, UCP2(−/−)-dispersed β-cells showed a faster and greater Ca^{2+} response to glucose than did those of WT mice (Fig. 6*A*). After treatment with palmitate, WT β-cells had increased basal cytosolic Ca^{2+} levels and an attenuated response to glucose, whereas UCP2(−/−) dispersed β-cells maintained their ability to respond to glucose (Fig. 6*B*). When UCP2(−/−) dispersed β-cells were transduced with AdUCP2, there was a reduction in the Ca^{2+} response after culture with either control or palmitate medium (Fig. 6*C*).

Insulin Secretion—Under control conditions, UCP2(−/−) islets showed enhanced GSIS compared with both control WT and UCP2(−/−) islets overexpressing UCP2 (Fig. 7). Basal insulin secretion was also elevated in UCP2(−/−) islets overexpressing UCP2 compared with WT islets. In addition, palmitate-treated WT islets and UCP2(−/−) islets overexpressing UCP2 had elevated basal insulin secretion and a blunted GSIS. On the contrary, UCP2(−/−) islets maintained the ability to secrete insulin in a glucose-dependent manner. In addition, UCP2(−/−) islets overexpressing UCP2 had a 50% reduction in GSIS under control medium conditions, and after treatment with palmitate there was a complete attenuation of glucose responsiveness (Fig. 7). AdEGFP had no effect on GSIS in control or palmitate-treated UCP2(−/−) islets, respectively (low glucose, 0.38 ± 0.11 and 0.13 ± 0.06 ng of insulin/μg of DNA; high glucose, 4.12 ± 0.33 and 3.42 ± 0.42 ng of insulin/μg of DNA; n = 4).

Reactive Oxygen Species Measurement—The level of oxidized DCF in islets was assessed by first determining DCF fluorescence in an islet and then moving away from the islet to measure the fluorescence of increasing amounts of oxidized DCF (Fig. 8*A*). Under control conditions, UCP2(−/−) islets had significantly elevated levels of oxidized DCF fluorescence compared with both WT and UCP2(−/−) islets overexpressing UCP2 (Fig. 8*B*). Palmitate exposure increased DCF fluorescence in WT and UCP2(−/−) islets overexpressing UCP2 but not in UCP2(−/−) islets (Fig. 8*B*).

DISCUSSION

Insulin secretion is enhanced in the absence of UCP2 (14) and attenuated when UCP2 is overexpressed (7). However, the physiologic role of UCP2 in the pancreatic β-cell is not well understood. The induction of UCP2 by a HFD or FFA exposure may contribute to β-cell lipotoxicity via suppression of GSIS. We showed that HFD-fed UCP2(−/−) mice or palmitate-treated UCP2(−/−) islets maintained pancreatic glucose responsiveness *in vivo* and *in vitro* compared with WT (Ref. 13 and present study). One explanation for the maintained glucose sensitivity in UCP2(−/−) islets is that higher FFA oxida-

tion prevents accumulation of TG in UCP2(−/−) islets, a phenomenon previously associated with lipotoxicity (30).

Treatment of islets with 0.4 mM palmitate increased UCP2 gene transcription and protein levels in WT islets and prevents glucose-induced hyperpolarization of the mitochondrial membrane potential ($\Delta\Psi_m$) and increases in the ATP/ADP. The reduced ability of glucose to hyperpolarize $\Delta\Psi_m$ is likely a key defect in the pathway leading to GSIS following palmitate exposure in WT islets and is consistent with uncoupling by UCP2. Alteration in $\Delta\Psi_m$ is an important event in ATP production in mitochondria; therefore it is not surprising that glucose was unable to stimulate an increase in the ATP/ADP ratio in WT islets. The ability of glucose to increase cytosolic Ca^{2+} was also attenuated in WT islets treated with palmitate, effects not seen in UCP2(−/−) islets. After palmitate treatment, UCP2 (−/−) islets show no loss in glucose-stimulated hyperpolarization of the $\Delta\Psi_m$, and they had maintained glucose-stimulated increases in the ATP/ADP and cytosolic Ca^{2+} levels. The net effect of palmitate treatment in WT islets was a reduction in GSIS, which does not occur in UCP2(−/−) islets.

In the present study we showed that uncoupling the mitochondria through UCP2 induction via palmitate or UCP2 overexpression attenuated ATP/ADP in the β-cell. These effects are the result of lipid treatment. However, we have also shown (18) that chronic treatment with glucose increased UCP2 mRNA and inhibited GSIS in WT islets via an increase in superoxide production. The superoxide-mediated loss in GSIS was prevented by overexpressing manganese superoxide dismutase in WT islets or by incubating WT islets with reagents that reduce superoxide such as Mn(III) tetrakis-(4-benzoic acid) porphyrin (MnTBAP) (18). MnTBAP is a membrane-permeable superoxide dismutase mimetic that can be loaded into islets to reduce superoxide. Superoxide is a known activator of UCP2 (5, 15), and reducing superoxide with manganese superoxide dismutase or MnTBAP attenuated UCP2 activity in WT islets. The ability of superoxide to prevent GSIS was not seen in UCP2(−/−) islets (18). It is interesting to point out that it is superoxide and not the H_2O_2 product of manganese superoxide dismutase or MnTBAP that modulates UCP2 activity because the overexpression of glutathione peroxidase-1, which converts H_2O_2 to H_2O, does not affect the ability of chronic hyperglycemia to reduce GSIS (18). In our studies UCP2(−/−) islets had elevated ROS, and this was reduced by UCP2 overexpression. Therefore, UCP2 may play a role in both lipotoxicity and glucotoxicity in the β-cell.

Overexpression of UCP2 using an adenoviral approach in UCP2(−/−) islets attenuated GSIS, an effect exacerbated by palmitate treatment. In addition, UCP2 overexpression in UCP2(−/−) islets also prevented glucose-stimulated hyperpolarization of $\Delta\Psi_m$ and the increase in cytosolic Ca^{2+}. Furthermore, whereas UCP2(−/−) islets overexpressing UCP2 had a 50% reduction in GSIS under control conditions, after treatment with palmitate there was complete inhibition of GSIS. This is consistent with previous data showing that β-cell UCP2 is activated by FFA via increased production of superoxide (31) and that superoxide induces UCP2-mediated uncoupling to suppress GSIS (18).

Excessive energy metabolism, as seen with lipid exposure, induces multiple adaptations that lead to cell damage, such as ceramide formation (32) and apoptosis in islets (33, 34). ROS are key players in β-cell apoptosis (34). Increased superoxide production is detrimental, in part, because the β-cell expresses low levels of antioxidant enzymes such as manganese superoxide dismutase (35). Why is there an elevation of UCP2 in β-cells if it is detrimental to β-cell glucose sensitivity? It may play a protective role in the pancreatic β-cell in response to increased metabolism-dependent superoxide production by dissipating excess energy flux thereby promoting β-cell survival under stress, such as a HFD. Further studies are required to determine whether this is the case. However, others have suggested that UCP2 plays a role in dissipating the excess energy flux generated by FFA metabolism and thus acts in a protective manner by reducing ROS production (5). Lack of UCP2 does lead to an elevation in ROS formation in macrophages from UCP2(−/−) mice (36) and in UCP2(−/−) islets (18), and there is a superoxide-mediated uncoupling of the mitochondria that occurs in a mouse clonal β-cell line, MIN6 cells (5), and pancreatic islets (18) that is likely mediated by UCP2.

In summary FFA-exposed pancreatic β-cells that lack UCP2 maintained glucose-stimulated hyperpolarization of the mitochondrial membrane potential and increases in the ATP/ADP ratio and cytosolic Ca^{2+} levels. This resulted in no attenuation of GSIS in response to fat treatment, suggesting that the lack of UCP2 may allow pancreatic β-cells to resist the detrimental effects of FFA. Overexpression of UCP2 into UCP2(−/−) islets resulted in a similar phenotype as that seen in WT islets exposed to palmitate; therefore it is possible that UCP2 plays a key role in fatty acid-induced abnormalities. Thus, inhibition of UCP2 activity may prove to be an effective treatment of glucose-intolerant individuals, but whether this would compromise β-cell survival is not known.

REFERENCES

1. Erecinska, M., Bryla, J., Michalik, M., Meglasson, M. D., and Nelson, D. (1992) *Biochim. Biophys. Acta* **1101,** 273–295
2. Boss, O., Hagen, T., and Lowell, B. B. (2000) *Diabetes* **49,** 143–156
3. Klingenberg, M., and Huang, S. G. (1999) *Biochim. Biophys. Acta* **1415,** 271–296
4. Echtay, K. S., Winkler, E., and Klingenberg, M. (2000) *Nature* **408,** 609–613
5. Echtay, K. S., Roussel, D., St Pierre, J., Jekabsons, M. B., Cadenas, S., Stuart, J. A., Harper, J. A., Roebuck, S. J., Morrison, A., Pickering, S., Clapham, J. C., and Brand, M. D. (2002) *Nature* **415,** 96–99
6. Krauss, S., Zhang, C. Y., and Lowell, B. B. (2002) *Proc. Natl. Acad. Sci. U. S. A.* **99,** 118–122
7. Chan, C. B., MacDonald, P. E., Saleh, M. C., Johns, D. C., Marban, E., and Wheeler, M. B. (1999) *Diabetes* **48,** 1482–1486
8. Esterbauer, H., Schneitler, C., Oberkofler, H., Ebenbichler, C., Paulweber, B., Sandhofer, F., Ladurner, G., Hell, E., Strosberg, A. D., Patsch, J. R., Krempler, F., and Patsch, W. (2001) *Nat. Genet.* **28,** 178–183
9. Sasahara, M., Nishi, M., Kawashima, H., Ueda, K., Sakagashira, S., Furuta, H., Matsumoto, E., Hanabusa, T., Sasaki, H., and Nanjo, K. (2004) *Diabetes* **53,** 482–485
10. Sesti, G., Cardellini, M., Marini, M. A., Frontoni, S., D'Adamo, M., Del Guerra, S., Lauro, D., De Nicolais, P., Sbraccia, P., Del Prato, S., Gambardella, S., Federici, M., Marchetti, P., and Lauro, R. (2003) *Diabetes* **52,** 1280–1283
11. Dhamrait, S. S., Stephens, J. W., Cooper, J. A., Acharya, J., Mani, A. R., Moore, K., Miller, G. J., Humphries, S. E., Hurel, S. J., and Montgomery, H. E. (2004) *Eur. Heart J.* **25,** 468–475
12. Hong, Y., Fink, B. D., Dillon, J. S., and Sivitz, W. I. (2001) *Endocrinology* **142,** 249–256
13. Joseph, J. W., Koshkin, V., Zhang, C. Y., Wang, J., Lowell, B. B., Chan, C. B., and Wheeler, M. B. (2002) *Diabetes* **51,** 3211–3219
14. Zhang, C. Y., Baffy, G., Perret, P., Krauss, S., Peroni, O., Grujic, D., Hagen, T., Vidal-Puig, A. J., Boss, O., Kim, Y. B., Zheng, X. X., Wheeler, M. B., Shulman, G. I., Chan, C. B., and Lowell, B. B. (2001) *Cell* **105,** 745–755
15. Echtay, K. S., Murphy, M. P., Smith, R. A., Talbot, D. A., and Brand, M. D. (2002) *J. Biol. Chem.* **277,** 47129–47135
16. Carlsson, C., Borg, L. A., and Welsh, N. (1999) *Endo* **140,** 3422–3428
17. Barbu, A., Welsh, N., and Saldeen, J. (2002) *Mol. Cell. Endocrinol.* **190,** 75–82
18. Krauss, S., Zhang, C. Y., Scorrano, L., Dalgaard, L. T., St Pierre, J., Grey, S. T., and Lowell, B. B. (2003) *J. Clin. Investig.* **112,** 1831–1842
19. Kang, G. X., Joseph, J. W., Chepurny, O. G., Monaco, M., Wheeler, M. B., Bos, J. L., Schwede, F., Genieser, H. G., and Holz, G. G. (2003) *J. Biol. Chem.* **278,** 8279–8285
20. Lacy, P. E., and Kostianovsky, M. (1967) *Diabetes* **16,** 35–39
21. Folch, J., Lees, M., and Sloane-Stanley, G. H. (1957) *J. Biol. Chem.* **226,** 497–509
22. Briaud, I., Harmon, J. S., Kelpe, C. L., Segu, V. B., and Poitout, V. (2001) *Diabetes* **50,** 315–321
23. Chen, S. Y., Ogawa, A., Ohneda, M., Unger, R. H., Foster, D. W., and McGarry, J. D. (1994) *Diabetes* **43,** 878–883
24. Smukler, S. R., Tang, L., Wheeler, M. B., and Salapatek, A. M. (2002) *Diabetes* **51,** 3450–3460
25. Drucker, D. J., Campos, R., Reynolds, R., Stobie, K., and Brubaker, P. L. (1991) *Endocrinology* **128,** 394–400
26. Schultz, V., Sussman, I., Bokvist, K., and Tornheim, K. (1993) *Anal. Biochem.* **215,** 302–304

27. Brubaker, P. L., Lee, Y. C., and Drucker, D. J. (1992) *J. Biol. Chem.* **267,** 20728–20733
28. Brubaker, P. L., So, D. C. Y., and Drucker, D. J. (1989) *Endocrinology* **124,** 3003–3009
29. Berts, A., Gylfe, E., and Hellman, B. (1995) *Biochem. Biophys. Res. Commun.* **208,** 644–649
30. Unger, R. H. (2002) *Annu. Rev. Med.* **53,** 319–336
31. Koshkin, V., Wang, X., Scherer, P. E., Chan, C. B., and Wheeler, M. B. (2003) *J. Biol. Chem.* **278,** 19709–19715
32. Unger, R. H., and Zhou, Y. T. (2001) *Diabetes* **50,** Suppl. 1**,** S118–S121
33. Shimabukuro, M., Zhou, Y. T., Levi, M., and Unger, R. H. (1998) *Proc. Natl. Acad. Sci. U. S. A.* **95,** 2498–2502
34. Chandra, J., Zhivotovsky, B., Zaitsev, S., Juntti-Berggren, L., Berggren, P. O., and Orrenius, S. (2001) *Diabetes* **50,** Suppl. 1**,** S44–S47
35. Lenzen, S., Drinkgern, J., and Tiedge, M. (1996) *Free Radic. Biol. Med.* **20,** 463–466
36. Arsenijevic, D., Onuma, H., Pecqueur, C., Raimbault, S., Manning, B. S., Miroux, B., Couplan, E., Alves-Guerra, M. C., Goubern, M., Surwit, R., Bouillaud, F., Richard, D., Collins, S., and Ricquier, D. (2000) *Nat. Genet.* **26,** 435–439

Free Fatty Acid-induced β-Cell Defects Are Dependent on Uncoupling Protein 2 Expression

Jamie W. Joseph, Vasilij Koshkin, Monique C. Saleh, William I. Sivitz, Chen-Yu Zhang, Bradford B. Lowell, Catherine B. Chan and Michael B. Wheeler

J. Biol. Chem. 2004, 279:51049-51056.
doi: 10.1074/jbc.M409189200 originally published online September 23, 2004
